

Studies on the de/re-hydrogenation characteristics of nanocrystalline MgH_2 admixed with carbon nanofibres

Rohit R. Shahi · Himanshu Raghubanshi ·
M. A. Shaz · O. N. Srivastava

Received: 8 November 2011 / Accepted: 6 March 2012 / Published online: 22 March 2012
© The Author(s) 2012. This article is published with open access at Springerlink.com

Abstract In the present investigation, we have synthesized different morphologies of carbon nanofibres (CNFs) to investigate their catalytic effect on the hydrogenation characteristics of 25 h ball-milled MgH_2 (nano MgH_2). The TEM analysis reveals that 25 h of ball-milling leads to the formation of nanocrystalline particles with size ranging between 10 and 20 nm. Different morphologies of CNFs were synthesized by catalytic thermal decomposition of acetylene (C_2H_2) gas over LaNi_5 alloy. Helical carbon nanofibres (HCNFs) were formed at a temperature 650 °C. By increasing the synthesis temperature to 750 °C, planar carbon nanofibres were formed. In order to explore the effectiveness of CNFs towards lowering the decomposition temperature, TPD experiments (at heating rate 5 °C/min) were performed for nano MgH_2 with and without CNFs. It was found that the decomposition temperature is reduced to ~334 and ~300 °C from 367 °C for the PCNF and HCNF catalysed nano MgH_2 . It is also found that HCNF admixed nano MgH_2 absorbs ~5.25 wt% within 10 min as compared with pristine nano MgH_2 , which absorbs only ~4.2 % within the same time and same condition of temperature and pressure. Thus the HCNF possesses better catalytic activity than PCNF. These different levels of improvement in hydrogenation properties of HCNF catalysed nano MgH_2 is attributed to the morphology of the CNFs.

Keywords Hydrogen storage materials · MgH_2 · Carbon nanostructures

Introduction

MgH_2 is a potential hydrogen storage material. It satisfies most of the requisites for a viable hydrogen storage system for mobile as well as stationary hydrogen devices. The slow hydriding and dehydriding are the major drawback of the magnesium hydride as hydrogen storage material. Bérubé et al. 2007, reported that the absorption at 600 K is initiated through the hydride formation at the Mg grain surface and that its rate of formation is controlled by the density of nucleation sites. The reaction would then stop when a hydride layer covers the surface of the magnesium preventing fast diffusion to the core of the particle and hence slowing down the kinetics of the β phase transition. Therefore, nano Mg may form a better material version for practical applications (Sakintuna and Lamari-Darkrim 2007). This leads to increase of surface area, creation of defects, and nucleation sites and also reduces the hydrogen diffusion path.

In order to further improve the sorption behaviour of MgH_2 , several studies have also reported that combination of ball-milling with a catalyst provides significant improvement in hydrogenation characteristics (Jain et al. 2010; Agarwal et al. 2009; Barkhordarian et al. 2006; Hanada et al. 2005; Charbonnier et al. 2004; Bobet et al. 2003; Zaluska et al. 2001; Tessier and Akiba 2000). The main drawback of these additives is the density of the metal and alloys which create a negative weight for storage applications. In recent years carbon nanostructures are being extensively used as a catalyst for improvement of the sorption behaviour of hydrogen storage materials (Wua and Cheng 2010).

Some recent reports have described MgH_2 admixed (catalysed) various carbon nanostructures (Imamura et al. 2003; Chen et al. 2004; Wu et al. 2005, 2006; Lillo-Ro'denas et al. 2008; Wu et al. 2010). These studies bring

R. R. Shahi (✉) · H. Raghubanshi · M. A. Shaz ·
O. N. Srivastava
Department of Physics, Hydrogen Energy Centre,
Banaras Hindu University, Varanasi 221005, India
e-mail: rohitrshahi@gmail.com

out the beneficial effect of carbon materials on both the hydriding and dehydriding behaviours. Among these results Wu et al. 2010 reported that 5 wt% SWCNTs catalysed MgH_2 absorbs 6 and 4.2 wt% of hydrogen at 423 and 373 K, respectively. However, Lillo-Ro'denas et al. 2008 investigated the effect of different carbon materials on decomposition of MgH_2 . The best results were achieved in the mixtures involving CNFs with metallic impurities (Ni and Fe). Wu et al. (2010) also reported that as prepared nickel-coated carbon nanofibres (NiCNF) exhibit a superior catalytic effect on hydrogenation behaviour of magnesium.

In the present investigation we have synthesized different morphologies of CNFs and investigated their catalytic effect on the hydrogenation behaviour of nano MgH_2 . Different morphologies of CNFs were synthesized by catalytic thermal decomposition of acetylene (C_2H_2) gas over LaNi_5 alloy at different temperature. The HCNFs were formed at a temperature 650 °C, whereas PCNFs were synthesized at temperature 750 °C.

Experimental details

The samples with and without the catalyst were characterized using powder X-ray diffraction (XRD) (X' Pert PRO, PANalytical) and transmission electron microscopy (TEM) (FEI, TECNAI 20G²). The XRD specimen holder was covered by a fine layer of parafilm (Pechiney plastic packing) for protecting the sample from air/moisture induced contamination. The hydrogen sorption behaviours of materials were analysed using the computerized Pressure-Concentration-Temperature (PCT) apparatus (AMC-USA).

Nanocrystalline MgH_2 (nano MgH_2) was synthesized through the ball milling of as received MgH_2 (particle size

is 50–100 μm as shown in SEM micrograph Fig. 1a) using Ritsh PM-400 ball miller. The milling was done under hydrogen (99.99 %) pressure of 5 atm for durations ranging from 5 to 35 h. It was found that the duration of 25 h is optimum for obtaining nano MgH_2 . Figure 1b is a representative SEM micrograph of 25 h ball-milled MgH_2 revealing the presence of particle size in the range of 500–1,000 nm (0.5–1 μm). It may be pointed out that the SEM analysis reveals the agglomeration of particles. The actual MgH_2 particles size as brought out by TEM ranges from 10 to 20 nm (as shown later in Fig. 7). It has been found that ball-milling under hydrogen pressure reduces the content of MgO. Ball-milling under hydrogen atmosphere reduces the oxide content due to the accelerated hydride formation over the surface of free Mg formed during ball milling (Bobet et al. 2003).

CNFs were synthesized by catalytic thermal decomposition of acetylene (C_2H_2) gas over LaNi_5 alloy. It has been optimized that the 100 mg of the catalyst is sufficient for each run in our experimental conditions. The details of the synthesis process have already been described by us (Raghubanshi et al. 2011). Helical carbon nanofibres (HCNFs) were formed at a temperature 650 °C. Figure 2a represents typical TEM micrograph of as synthesized HCNF. This shows that the as grown CNFs have helical morphology and their typical diameter is 150 nm (shown in Fig. 2a). By increasing the synthesis temperature to 750 °C, planar carbon nanofibres (diameter 200 nm) were formed as shown in Fig. 2b. In both the cases the length of CNFs was 6–8 μm .

Admixing of CNFs were performed inside the glove box using locally fabricated mixer (at 4000 rpm) having three chromium nickel stainless steel balls (2 balls of weight 8.5 g, and 1 ball of weight 0.25 g) and vial having a

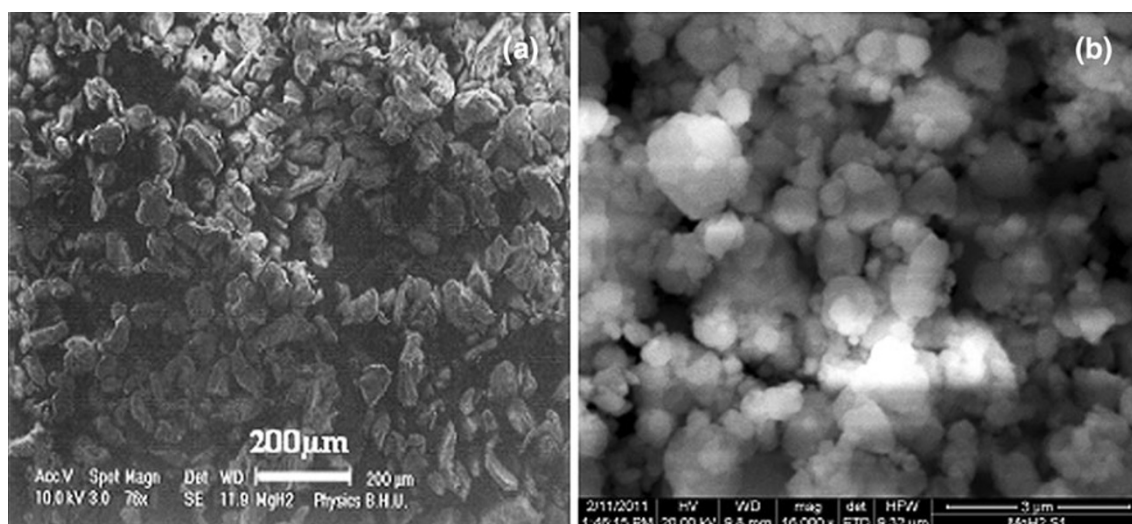


Fig. 1 SEM micrograph of **a** as received MgH_2 , **b** 25 h ball-milled MgH_2 under 5 atm of hydrogen pressure

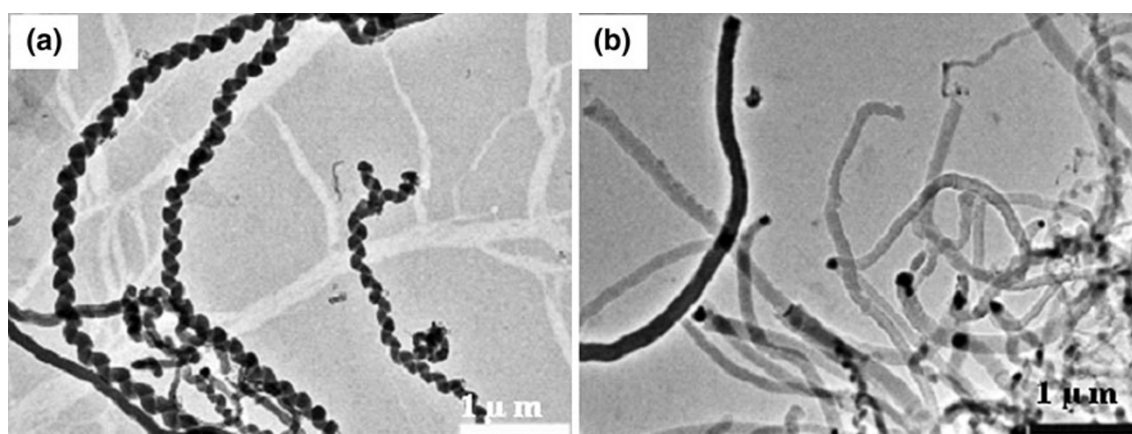


Fig. 2 TEM micrograph of **a** as synthesized HCNF, **b** as synthesized PCNF

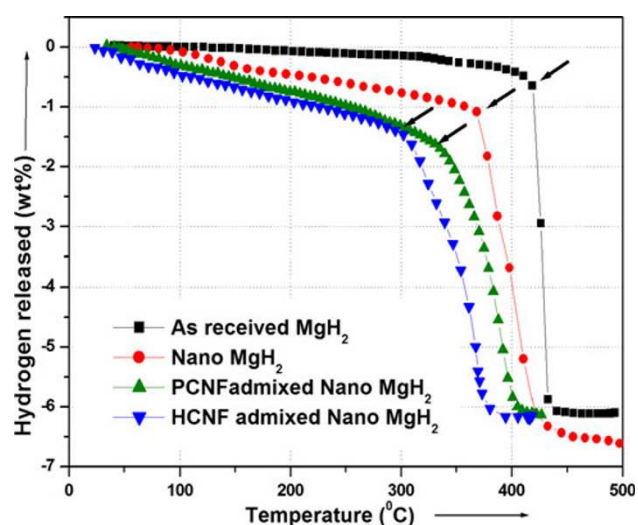


Fig. 3 TPD profile of as received MgH_2 , nano MgH_2 with and without CNF at heating rate $5\text{ }^\circ\text{C}/\text{min}$

volume of 150 cc (Shahi et al. 2012). This is beneficial since it is known that morphology of carbon nanostructure (CNS) is important in regard to their catalytic activity; the aforementioned method of admixing maintains the structural morphology of admixed CNS, which acts as a catalyst for hydrogenation/dehydrogenation of nano MgH_2 . By varying the concentration of CNF being admixed in nano MgH_2 it is found that the optimum concentration of CNF is 2 wt%.

Results and discussion

Hydrogenation dehydrogenation characteristics of nano MgH_2 with and without CNF

In order to investigate the effect of ball-milling and the catalytic effect of CNF, the temperature programmed

desorption (TPD) experiments were performed on the nano MgH_2 with and without CNF. Figure 3 represents the decomposition profile at a heating rate of $5\text{ }^\circ\text{C}/\text{min}$ for as received MgH_2 , nano MgH_2 , PCNF and HCNF admixed nano MgH_2 . TPD curves reveal that the decomposition temperature of as received MgH_2 is reduced appreciably with ball-milling for 25 h. It illustrates that the as received MgH_2 has a sharp decomposition at temperature $422\text{ }^\circ\text{C}$. The decomposition temperature is reduced to $367\text{ }^\circ\text{C}$ for ball-milled MgH_2 . Thus ball-milling reduces the decomposition temperature up to $\sim 55\text{ }^\circ\text{C}$. The decrease in temperature has been outlined by the arrow in Fig. 3. As can be seen from figure the decomposition temperature is reduced to ~ 334 and $\sim 300\text{ }^\circ\text{C}$ for the PCNF and HCNF admixed nano MgH_2 . Thus the decomposition temperature of nano MgH_2 is reduced to ~ 300 from $\sim 367\text{ }^\circ\text{C}$ with admixing of HCNF. It can thus be said that the TPD experiment reveals that the HCNF catalysed nano MgH_2 has $\sim 67\text{ }^\circ\text{C}$ lower decomposition temperature as compared with pristine nano MgH_2 . It may be pointed out that the effect of ball milling itself reduces the desorption temperature from 422 to $367\text{ }^\circ\text{C}$. A further decrease of $67\text{ }^\circ\text{C}$ takes place due to catalytic effect of HCNF. Thus in comparison with the as received MgH_2 there is a total decrease of $122\text{ }^\circ\text{C}$ in desorption temperature.

In order to further investigate the catalytic activity of CNF, the isothermal absorption kinetics measurements were also performed for the nano MgH_2 with and without CNF. The absorption kinetics plots for nano MgH_2 with and without CNF at $300\text{ }^\circ\text{C}$ and 2 MPa of hydrogen pressure are shown in Fig. 4. The hydrogen uptake capacity of nano MgH_2 is found to be 4.8 wt%. This gets improved with admixing of PCNFs and HCNFs. It is found that the nano MgH_2 admixed with PCNF and HCNF absorbs 5.7 and 5.8 wt% of hydrogen, respectively, within 1 h. It is also found that HCNF admixed nano MgH_2 absorbs ~ 5.25 wt% within 10 min as compared with pristine nano

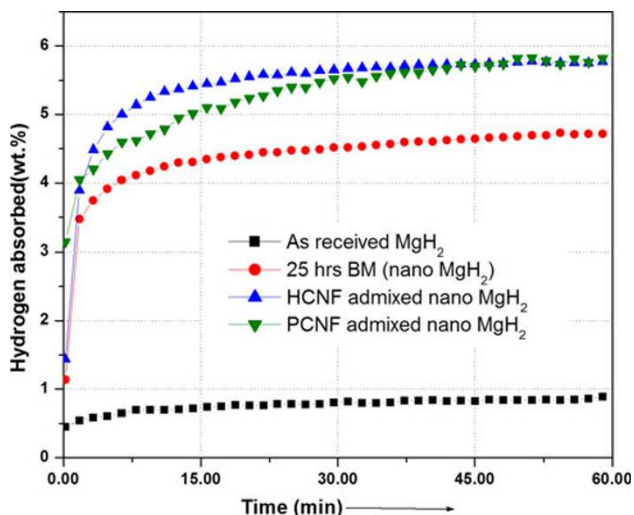


Fig. 4 Absorption kinetics plots of as received MgH₂, nano MgH₂ with and without CNF at 300 °C and 20 MPa of hydrogen pressure

MgH₂, which absorbs only ~4.2 % within the same time and same condition of temperature and pressure. Thus absorption kinetics of the pristine nano MgH₂ improves significantly with admixing of HCNF.

Evaluation of activation energy for absorption of nano MgH₂ with and without HCNFs

As a further step towards understanding rehydrogenation, the activation energy *E_a* for hydrogen absorption of nano MgH₂ as well as the HCNF catalysed nano MgH₂ has been calculated. The activation energy for hydrogen absorption was estimated from Arrhenius plots. This is calculated from the following equation:

$$k = Ae^{-E_a/RT}$$

where *k* is the rate constant, *R* is gas constant, *T* is temperature at which absorption experiment is performed.

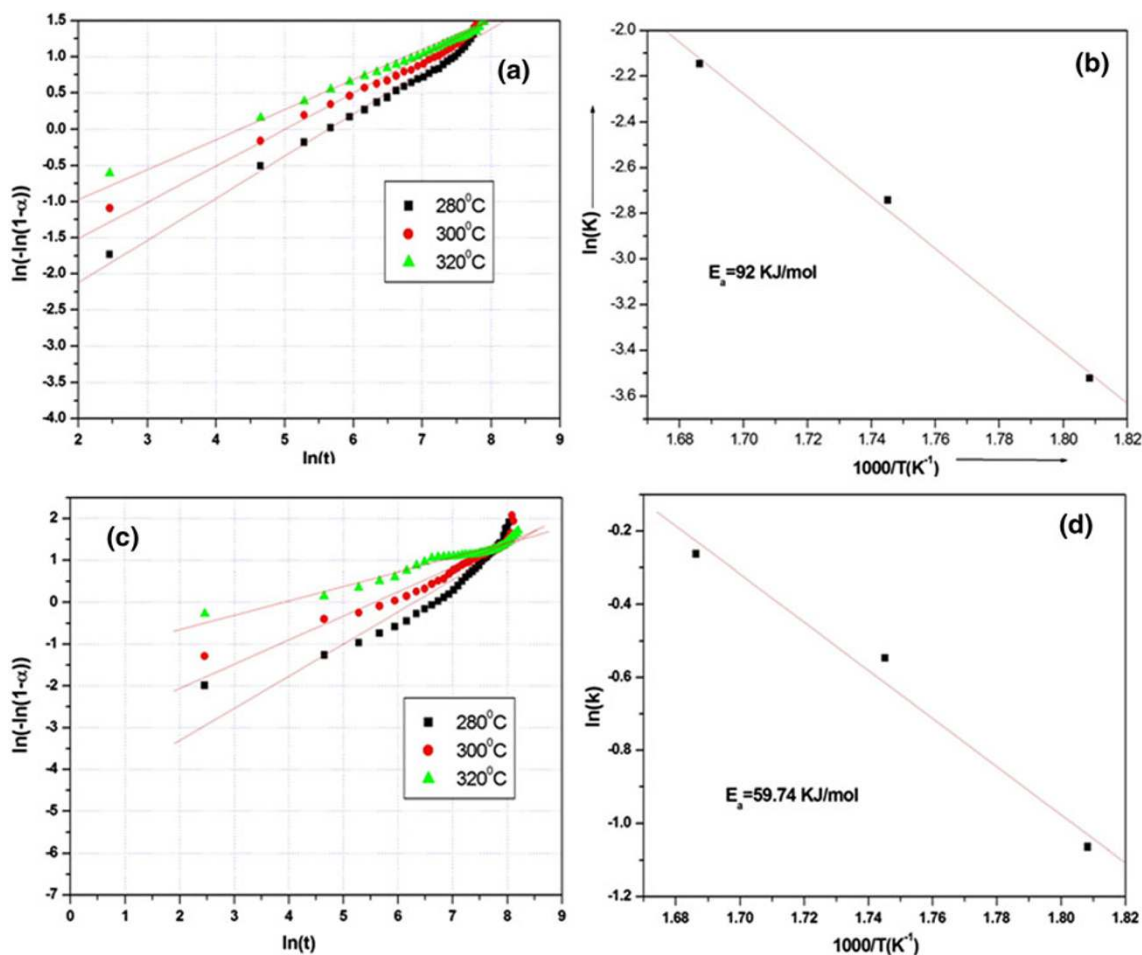


Fig. 5 **a** Plot of $\ln[-\ln(1-\alpha)]$ versus $\ln(t)$ for nano MgH₂, **b** Arrhenius plot $\ln(k)$ versus $1,000/T$ for nano MgH₂, **c** plot of $\ln[-\ln(1-\alpha)]$ versus $\ln(t)$ for HCNF admixed nano MgH₂ **d** Arrhenius plot $\ln(k)$ versus $1,000/T$ for HCNF admixed nano MgH₂

The absorption curve for MgH_2 is not linear; therefore the rate constant k was obtained using the John-Mehl-Avrani model (Avrami 1941). This proposed kinetic model

for nucleation and growth in solids is outlined by the following equation:

$$-\ln(1 - \alpha)^{1/n} = kt$$

where α is the extent of the reaction which can be identified with a normalized hydrogen wt% (range from 0 to 1), t is time and for a fixed temperature k and n are constant.

Figure 5a represents the plot of $\ln[-\ln(1-\alpha)]$ versus $\ln(t)$ for different temperatures; the slope of these plots gives $\ln k$. Further the slope of the Arrhenius plot ($\ln k$ vs. $1/T$) Fig. 5b gives activation energy. The E_a is found to be 92 kJ/mol for nano MgH_2 . However, for the as received MgH_2 , the activation energy was found to be 98 kJ/mol [as described in our previous report (Singh et al. 2010)]. Similar method is adopted for the evaluation of activation energy for HCNF admixed nano MgH_2 . Figure 5c and d describes the results of evaluation of HCNF catalysed nano MgH_2 ; the activation energy is found to be 59.7 kJ/mol.

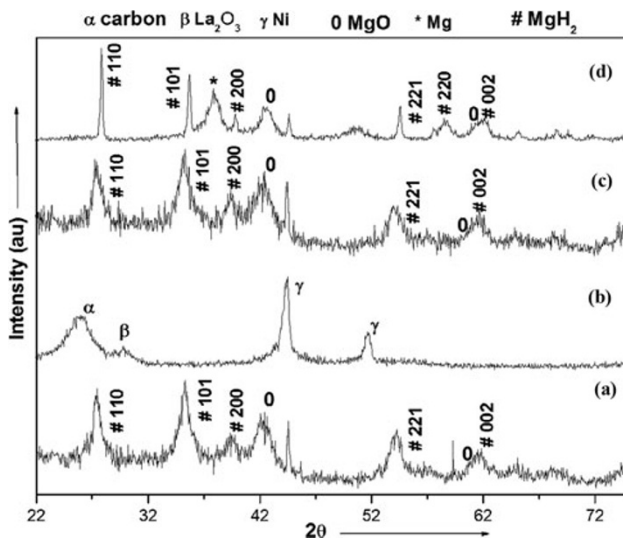


Fig. 6 XRD patterns of **a** 25 h ball-milled MgH_2 , **b** as synthesized HCNF, **c** HCNF admixed nano MgH_2 and **d** rehydrogenated HCNF admixed nano MgH_2

Structural and microstructural characterization of CNF catalysed nano MgH_2

To make these changes explicable, the structure and morphology of the HCNF admixed nano MgH_2 is examined by

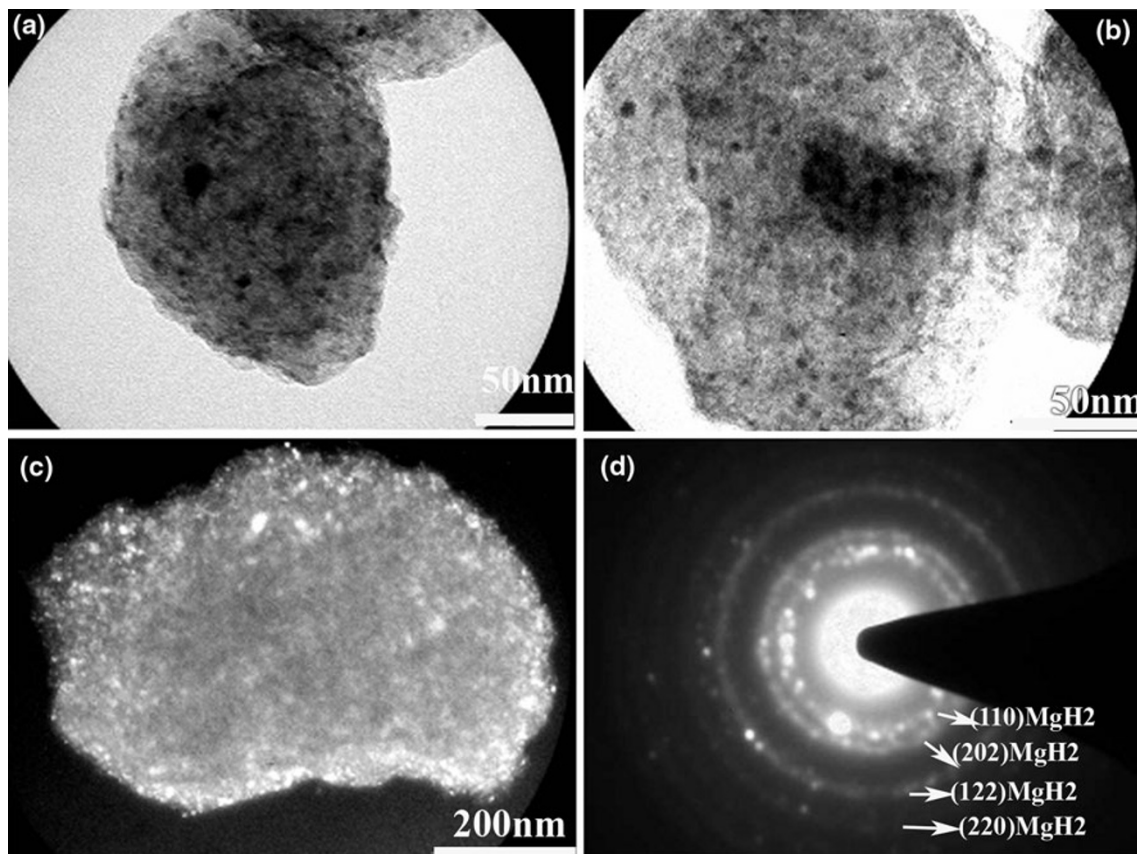


Fig. 7 TEM micrograph **a**, **b** at 50 nm scale **c** dark field micrograph **d** SADP of 25 h ball-milled MgH_2

employing XRD and TEM. Figure 6 brings out representative X-ray diffraction patterns of the (a) as synthesized nano MgH_2 , (b) as synthesized HCNF, (c) HCNF catalysed nano MgH_2 and (d) rehydrogenated HCNF catalysed nano MgH_2 . As can be seen from Fig. 6a, the XRD peaks exhibit considerable broadening. The crystallite size for the nano MgH_2 is found to be 10 nm calculated through the Scherrer formula. TEM micrograph (Shown in Fig. 7) also reveals a similar crystallite size distribution. The formation of nano MgH_2 through the ball milling is thus evident. The typical XRD pattern of the as synthesized HCNF (Fig. 6b) shows typical graphite XRD peaks (indexed in the figure) together with the synthesis acquired metallic Ni particle. Fig. 6c brings out a representative X-ray diffraction pattern of HCNF admixed nano MgH_2 ; it can be noticed that the peaks corresponding to MgH_2 alone are present. Since the catalyst is in very small concentration, it will not be discernible in the XRD pattern.

In order to further understand the morphological changes with admixing of HCNF in nano MgH_2 , transmission electron microscope studies of the as synthesized nano MgH_2 and HCNF catalysed nano MgH_2 (which showed the optimum hydrogenation behaviour) are carried out. Figure 7a and b exhibit typical TEM micrograph of the as synthesized (25 h ball milled) nano MgH_2 . It is found that the synthesized nano MgH_2 has particles in the range of 10–20 nm as evident from TEM micrograph. This feature is more clearly visible in the dark field micrograph of synthesized nano MgH_2 shown in Fig. 7c. The corresponding electron diffraction pattern obtained from the nano MgH_2 is shown in Fig. 7d. The spotty rings were indexed based on the tetragonal structure of βMgH_2 .

Figure 8a, on the other hand, exhibits representative TEM micrograph of HCNF catalysed nano MgH_2 . From the microstructure, the presence of CNF can be verified. The microstructure also reveals that HCNFs are dispersed nearly homogeneously in nano MgH_2 . The selected area electron diffraction pattern representing the microstructure is shown in Fig. 8b. The presence of diagonally opposite arced diffraction spots is signatures of HCNF admixed in nano MgH_2 other signs are similar to those shown in Fig. 7d are representing nano MgH_2 .

The XRD pattern of synthesized CNF revealed that the CNF contained Ni-metallic nano particles as impurity. Thus the catalytic activity of these CNFs may also arise due to the presence of synthesis acquired metal nano particles. In order to understand the influence of Ni-nanoparticles on the catalytic activities of CNFs, we have further investigated the dehydrogenation characteristics of nano MgH_2 catalysed separately with Ni-nano particles and purified CNFs. Purification (acid treatment) of as synthesized CNF has been performed with the concentrated HNO_3 and washed with distilled water several times. After

the acid treatment, it has been found that the morphology of the CNF has not changed; only the concentration of metallic particle becomes negligible (Raghubanshi et al. 2011). From the TPD experiments it has been found that dehydrogenation temperatures for nano MgH_2 catalysed separately with purified CNF and Ni-nano particles are 350 and 360 °C, respectively (not shown here), whereas for the case of pristine nano MgH_2 , the dehydrogenation temperature is found to be 367 °C. Thus the admixing of purified CNF and Ni-nano particle shows only marginal change in dehydrogenation temperature. However, the dehydrogenation temperature of as synthesized PCNF catalysed nano MgH_2 is found to be 334 °C. Hence for the present case the combined effect (embedded Ni-nano particles and fibrous morphologies of CNF) is responsible for the catalytic effect of the as synthesized CNFs. Moreover, HCNF possess better catalytic activity as compared with PCNFs since both the CNFs (PCNF and HCNF) have similar synthesised metal nanoparticles (Ni). Hence these different levels of improvement in hydrogenation behaviour of PCNF and HCNF catalysed nano MgH_2 may arise due the

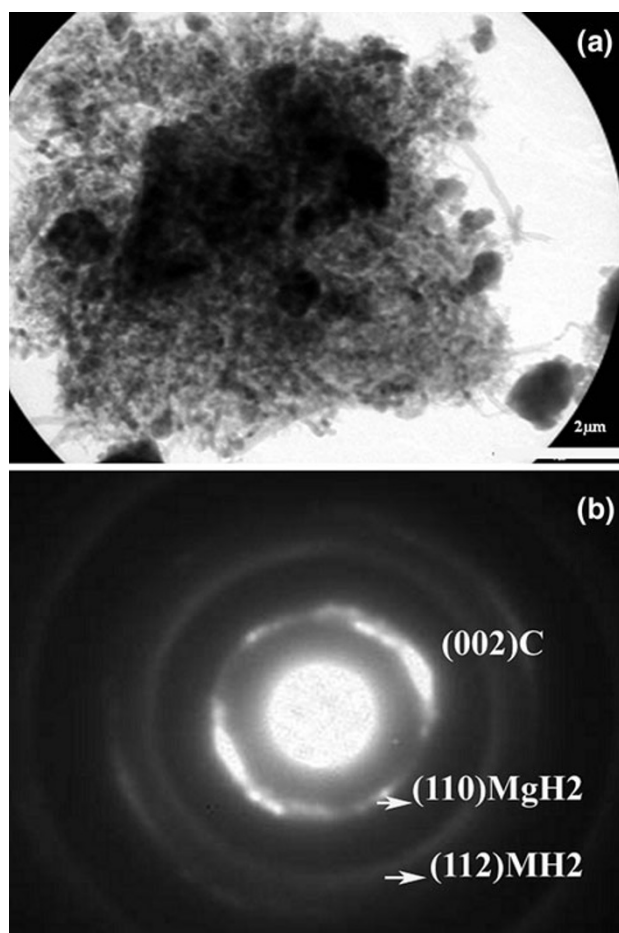


Fig. 8 TEM micrograph of **a** HCNF admixed nano MgH_2 **b** SADP of admixed sample

morphological differences of these two CNFs. Berseth et al. (2009) have also reported that the electronegativity of carbon nanostructures increases with increasing the curvature of carbon nanostructures. Among these CNFs (PCNF and HCNF), the curvature of the HCNFs may increase the electronegativity of HCNFs as compared with PCNFs. Hence for the case of HCNF catalysed nano MgH_2 , the bonding electrons present in MgH_2 may become more delocalized as compared with PCNF catalysed nano MgH_2 due to the electronegativity difference between these two CNFs.

Conclusions

The de/re-hydrogenation characteristics of nano MgH_2 is improved significantly with admixing of carbon nanofibres. The lowering of decomposition temperature for CNFs catalysed samples as compared with pristine nano MgH_2 is from ~ 367 to ~ 334 °C and ~ 300 °C for PCNF and HCNF catalysed nano MgH_2 , respectively. Thus HCNF possesses better catalytic activity as compared with PCNF. It is also found that the activation energy for rehydrogenation of HCNF catalysed nano MgH_2 is ~ 59.7 kJ/mol, whereas the activation energy for rehydrogenation of pristine nano MgH_2 is ~ 92 kJ/mol. These different levels of improvement in hydrogenation properties of CNF catalysed nano MgH_2 is attributed to the morphological differences of these CNFs.

Acknowledgments The authors would like to acknowledge Prof. R.S. Tiwari for his encouragement and helpful discussion. Financial assistance received from Ministry of New and Renewable Energy (MNRE), DST (UNANST), UGC-New Delhi (India) and Council of Scientific and Industrial Research (CSIR) is gratefully acknowledged. One of the authors (Mr. Rohit R. Shahi) acknowledges Dr. Kalpana Awasthi for her helpful suggestions.

Open Access This article is distributed under the terms of the Creative Commons Attribution License which permits any use, distribution, and reproduction in any medium, provided the original author(s) and the source are credited.

References

Agarwal S, Aurora A, Jain A, Jain IP (2009) Montone A catalytic effect of ZrCrNi alloy on hydriding properties of MgH_2 . *Int J Hydrogen Energy* 34:9157–9162

Avrami M (1941) Kinetics of phase change granulation, phase change and microstructures. *J Chem Phys* 9:177

Barkhordarian G, Klassen T, Bormann R (2006) Kinetic investigation of the effect of milling time on the hydrogen sorption reaction of magnesium catalyzed with different Nb_2O_5 contents. *J Alloys Compd* 407:249–255

Berseth PA, Harter AG, Zidan R, Blomqvist A, Araujo CM, Scheicher RH et al (2009) Carbon nanomaterials as catalysts for hydrogen uptake and release in NaAlH_4 . *Nano Lett* 9:1501–1505

Bérubé B, Radtke G, Dresselhaus M, Chen G (2007) Size effects on the hydrogen storage properties of nanostructured metal hydrides: a review. *Int J Hydrogen Energy Res* 31:637–663

Bobet JL, Desmoulins-Krawiec S, Grigorova E, Cansell F, Chevalier B (2003) Addition of nanosized Cr_2O_3 to magnesium for improvement of the hydrogen sorption properties. *J Alloys Compd* 351:217–221

Charbonnier J, de Rango P, Fruchart D, Miraglia S, Pontonnier L, Rivoirard S, Skryabina N, Vulliet P (2004) Hydrogenation of transition element additives (Ti, V) during ball milling of magnesium hydride. *J Alloys Compd* 383:205–208

Chen D, Chen L, Liu S, Ma CX, Chen DM, Wang LB (2004) Microstructure and hydrogen storage property of Mg/MWNTs composites. *J Alloys Compd* 372:231–237

Hanada N, Ichikawa T, Fujii H (2005) Catalytic effect of nanoparticle 3d-transition metals on hydrogen storage properties in magnesium hydride MgH_2 prepared by mechanical milling. *J Phys Chem B* 109:7188–7194

Imamura H, Kusuhara M, Minami S, Matsumoto M, Masanari K, Sakata Y, Itoh K, Fukunaga T (2003) Carbon nanocomposites synthesized by high-energy mechanical milling of graphite and magnesium for hydrogen storage. *Acta Mat* 51:6407–6414

Jain IP, Lal C, Jain A (2010) Hydrogen storage in Mg: a most promising material. *Int J Hydrogen Energy* 35:5133–5144

Lillo-Ro'denas MA, Aguey-Zinsou KF, Cazorla-Amoro's D, Linares-Solano A, Guo ZX (2008) Effect of different carbon materials on MgH_2 decomposition. *Carbon* 46:126–137

Raghubanshi H, Hudson MSL, Srivastava ON (2011) Synthesis of helical carbon nanofibres and its application in hydrogen desorption. *Int J Hydrogen Energy* 36:4482–4490

Sakintuna B, Lamari-Darkrim F, Hirscher M (2007) Metal hydride materials for solid hydrogen storage: a review. *Int J Hydrogen Energy* 32:1121–1140

Shahi RR, Raghubanshi H, Shaz MA, Srivastava ON (2012) Studies on the de/rehydrogenation characteristic of $\text{Mg}(\text{NH}_2)_2/\text{LiH}$ mixture admixed with carbon nanofibres. *Int J Hydrogen Energy* 37:3705–3711

Singh RK, Raghubanshi H, Pandey SK, Srivastava ON (2010) Effect of mixing different carbon structural variants on the decomposition and hydrogen sorption kinetics of magnesium hydride. *Int J Hydrogen Energy* 35:4131–4137

Tessier P, Akiba E (2000) Decomposition of nickel-doped magnesium hydride prepared by reactive mechanical alloying. *J Alloys Compd* 30:215–217

Wu C, Wang P, Yao X, Liu C, Chen D, Lu GQ, Cheng H (2005) Effects of SWNT and metallic catalyst on hydrogen absorption/desorption performance of MgH_2 . *J Phys Chem B* 109:22217–22221

Wu C, Wang P, Yao X, Liu C, Chen D, Lu GQ, Cheng H (2006) Effect of carbon/noncarbon addition on hydrogen storage behaviours of Magnesium hydride. *J Alloys Compd* 414:256–2264

Wu CZ, Yao XD, Zhang H (2010) Hydriding/dehydriding properties of $\text{MgH}_2/5$ wt% Ni coated CNFs composite. *Int J Hydrogen Energy* 35:247–252

Wua C, Cheng HM (2010) Effects of carbon on hydrogen storage performances of hydrides. *J Mater Chem* 20:5390–5400

Zaluska A, Zalusk L, Ström-Olsen JO (2001) Structure, catalysis and atomic reactions on the nano-scale: a systematic approach to metal hydrides for hydrogen storage. *App Phys A: Mat Sci Proc* 72:157–165